ANNALI DI GEOFISICA, VOL. XXXVII, N. 6, December 1994

Broad-band moment tensor inversion from single station, regional surface waves for the 1990, NW-Iran earthquake sequence

Domenico Giardini([1]), **Luca Malagnini**([2]), **Barbara Palombo**([2]) **and Enzo Boschi**([2])
([1]) *Dipartimento di Scienze Geologiche, III Università di Roma, Italy*
([2]) *Istituto Nazionale di Geofisica, Roma, Italy*

Abstract
We present a method for the inversion of complete waveforms in the 5-30 mHz frequency band for moment tensor determination. The method is based on the calibration of phase and group velocity dispersion curves for Rayleigh and Love fundamental modes to account for heterogeneous lithospheric structure, and is applied to the analysis of single station records of the VSL MEDNET station for the 1990 NW Iran earthquake sequence (the events of June 20, 21 and 24). The revised seismic moment of the June 20, 1990 Iranian earthquake is $M_0 = 1.56 \times 10^{27}$ dyne-cm, corresponding to $M_w = 7.4$. The method proves to be a very robust tool for the analysis of moderate and large earthquakes at regional distances, producing consistent moment tensor solutions from single station inversions in narrow (2-4 mHz) and wide (up to 20 mHz) frequency bands across the whole band of interest.

Key words *seismic moment – inversion techniques – regional waveform analysis – 1990 NW-Iran seismicity*

1. Introduction

The deployment of global digital seismic networks (GSN, IDA, GEOSCOPE), of regional networks in all continents (MEDNET, CDSN, CNSN, MIDAS, USNSN, ADSN) and of arrays at national or more local scale (for example the networks installed in California by TERRAscope, UCSC and UCB) provide a wealth of high-quality waveforms, (see Boschi *et al.*, 1991, for a review of regional and global digital networks).

Moment tensor catalogues have been compiled for more than 11 000 events since 1977, chiefly by Harvard University using the CMT method of Dziewonski *et al.*, (1981), replacing traditional earthquake catalogues as the primary tool of seismotectonic analysis. Methods for moment tensor inversion have been proposed using global data (Dziewonski *et al.*, 1981; Kanamori and Given, 1981; Sipkin, 1986; Romanowicz and Suarez, 1983; Giardini, 1992) and more recently also regional waveforms (Holt and Wallace, 1987; Fukushina *et al.*, 1989; Dreger and Helmberger, 1990; Nakanishi *et al.*, 1992; Ritsema and Lay, 1993; Giardini *et al.*, 1993; Romanowicz *et al.*, 1993; Thio and Kanamori, 1995); some methods deal specifically with single station inversions (Ekström *et al.*, 1986; Jimenez *et al.*, 1989; Dufumier and Cara, 1995; Giardini *et al.*, 1995). Quasi-real time moment tensor inversion is now routinely carried out by several groups for global earthquakes (Harvard, NEIS, Caltech, ERI) and

for local and regional earthquakes (Caltech, UCSC, UCB, ING, ERI).

Modelling complete long-period regional waveforms (in the 100-3000 km distance range and 30-200 s period range) is a complex exercise, due to theoretical and practical limitations. Body and surface waves overlap in time in the seismogram at close distances, posing serious problems of separation and modelling; body waves can be modelled using a standard stratified model, while surface waves require the accurate calibration of dispersion curves, which have been calibrated with sufficient accuracy only in very few locations around the world.

The aim of this work is to develop algorithms for moment tensor inversion in the 5-30 mHz wide frequency band, using complete three-component waveform records and calibrating dispersion curves of phase velocity for fundamental Rayleigh and Love waves; while the dispersion curves can be classically used in an inversion scheme (*e.g.* a pure-path method) for the determination of the velocity structure, we are interested here in their application in waveform inversions for source analysis and we test two different approaches to the determination of group and phase velocity calibrations. A second goal is to verify the accuracy of single-station moment tensor determinations in narrow-band and wide-band inversions for application in routine monitoring of seismic sequences and regional seismicity.

We present moment tensor determinations for the mainshock and largest aftershocks of the June 1990 sequence in Northwestern Iran, expanding waveform inversion techniques proposed for the quantification of regional and global earthquakes (Giardini, 1992; Giardini *et al.*, 1993; Giardini *et al.*, 1995).

We use waveforms recorded by MEDNET, the very-broad-band seismographic network installed by the Istituto Nazionale di Geofisica of Roma in countries of the Mediterranean area, in the framework of the WorldLab program Plato-I (Boschi *et al.*, 1991). The high standards of the VBB technology and of the MEDNET installation procedures (Giardini *et al.*, 1992) allow Earth noise in the low-frequency band and wave trains with excellent signal-to-noise ratios to be recorded at regional distances for small earthquakes (m = 4-5); the best performance in the long-period band is obtained in the 40-130 s period range.

2. The 1990 NW-Iran earthquake sequence

The Rudbar-Tarom or Manjil earthquake of June 20, 1990 occurred in the Western Alborz mountain belt in Northwestern Iran, southwest of the Caspian Sea (Moinfar and Naderzadeh, 1990; Berberian *et al.*, 1992). With magnitude $M_S = 7.6$ and moment $M_0 = 1.56 \times 10^{27}$ dyne-cm ($M_W = 7.4$), it was the largest earthquake to hit that area in hystorical times, killing more than 40000 people and destroying three cities and 700 villages. Surface faulting and folding were observed in the epicentral area; three main segments of co-seismic surface break were observed, for a total length of at least 80 km and with maximum left-lateral displacement of 60 cm. Two large aftershocks took place on June 21 ($M_W = 5.7$) and June 24 ($M_W = 5.3$).

Figure 1 (modified after Berberian *et al.*, 1992) shows a map of the epicentral area of the 1990 NW-Iran earthquake sequence, the macroseismic fields of intensity larger than MCS = VII, the surface faulting, the location and mechanisms of the June 20 mainshock and the June 21 and 24 aftershocks determined in this study.

To obtain a moment tensor solution for the June 20 mainshock, following Giardini (1992) we invert 6 hours of three-component waveforms recorded by the MEDNET stations of MDT, VSL, AQU and BNI, band-passed in the 5-7 mHz frequency band, using as kernels complete synthetic seismograms computed by normal modes summation (Woodhouse, 1988) using PREM (Dziewonski and Anderson, 1981); waveform modelling for station MDT is shown in fig. 2.

Our scheme accounts for the centroid time and location of the event by computing iteratively a time correction for each station; the centroid depth is constrained by minimizing the variance of inversions with different trial depths (*cfr.* Romanowicz and Suarez, 1983).

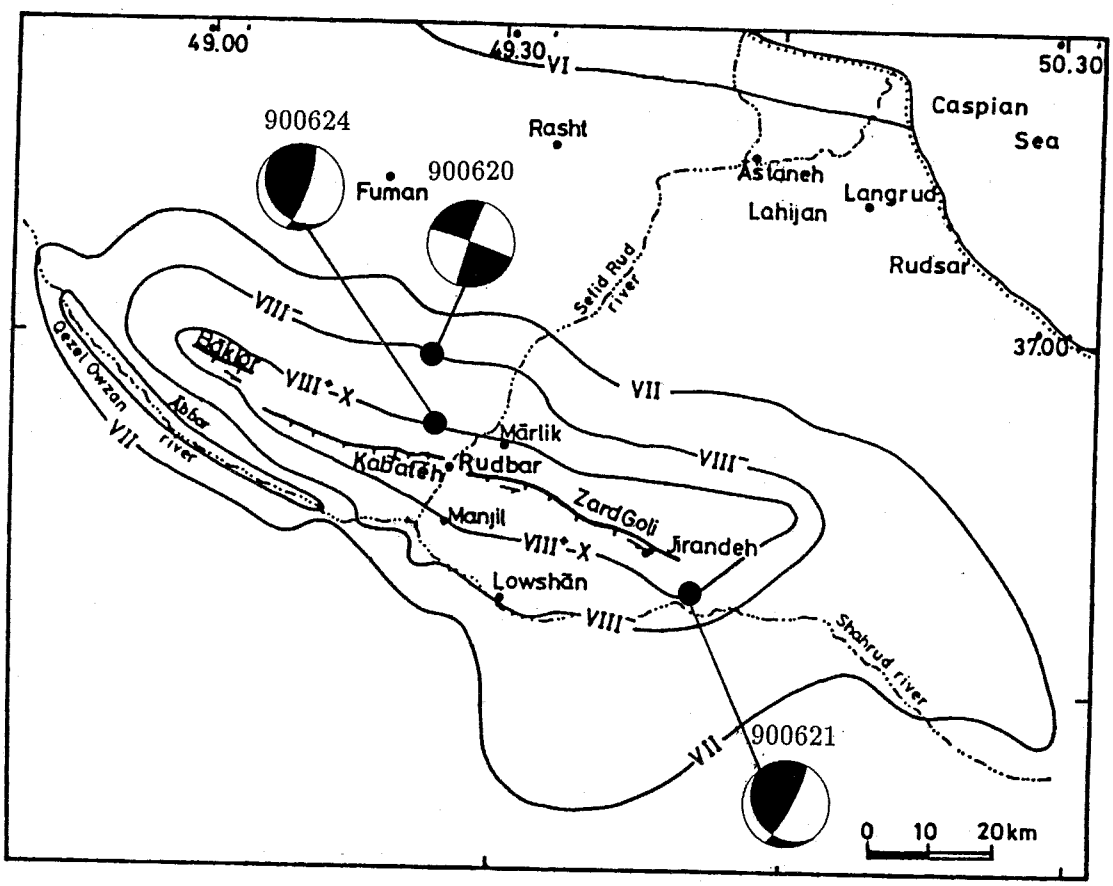

Fig. 1. The 1990 NW-Iran earthquake sequence. We display the epicentral area, the macroseismic fields of intensity larger than MCS = VI, the surface trace of the earthquake fault break (modified from Berberian *et al.*, 1992) the mechanisms of the mainshock (June 20, 1990) and the two aftershocks used in this study (June 21 and 24, 1990).

Figure 3 shows the normalized variance and the seismic moment obtained at different trial depths; while the variance is insensitive to the hypocentral depth, the seismic moment increases at depths below 35 km constraining the hypocentral depth in the first 30 km.

The seismic moment (1.1×10^{27} dyne-cm) and the almost pure strike-slip mechanism with a fault plane striking WNW are in agreement with the CMT solutions obtained by Harvard (1.35×10^{27} dyne-cm; Dziewonski *et al.*, 1991), NEIS (1.1×10^{27} dyne-cm), Caltech (1.0×10^{27} dyne-cm; Thio *et al.*, 1990) and by Berberian *et al.* 1992; 8.8×10^{26} dyne-cm) (see also Giardini, 1992).

3. A scheme to model regional waveforms

The analysis of earthquakes of moderate size (M_W = 4-6) requires the modelling of body and surface waveforms in the 10-30 mHz frequency range. Body waves can be modelled in amplitude and phase in the 10-30 mHz band

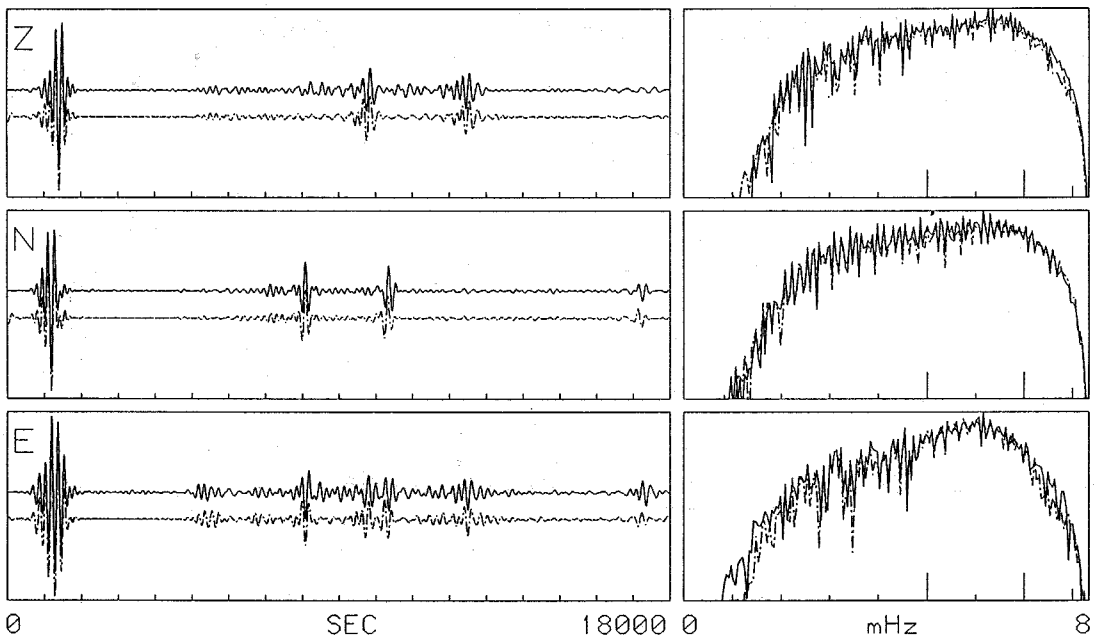

Fig. 2. Long-period waveform modelling for station MDT for the June 20, 1990 Iranian mainshock. On the left are displayed six hours of three-components time series (V,N,E); data are indicated by continuous lines, synthetic seismograms by dashed lines. On the right are the corresponding amplitude spectra, tapered at high and low frequencies. The frequency band used in the inversion for the moment tensor is marked (5-7 mHz) (modified from Giardini, 1992).

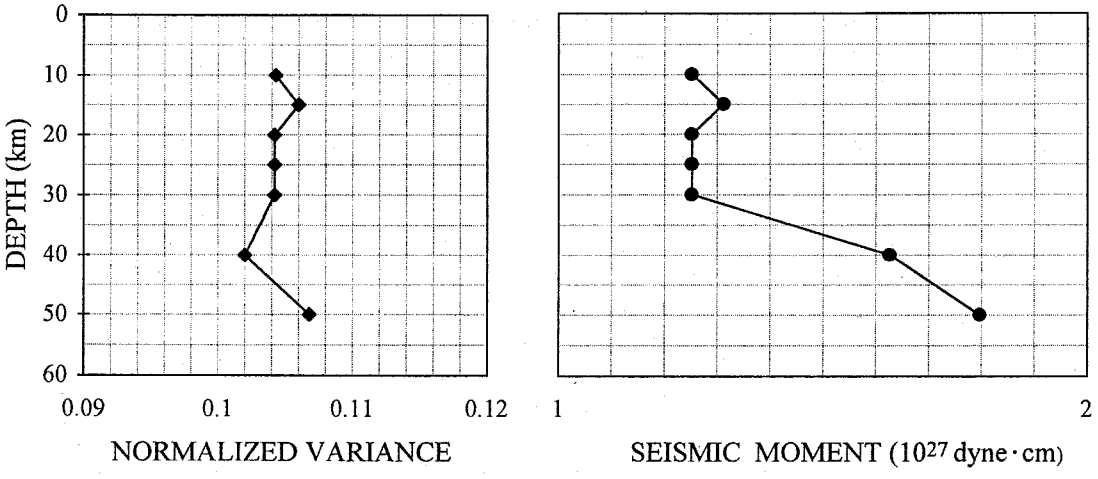

Fig. 3. Normalized variance, defined as the ratio between the misfit and the data, and seismic moment obtained in moment tensor inversions at different trial depths for the June 20, 1990 Iranian mainshock.

using a standard stratified model; the amplitude of surface waves can be reproduced by an average structural model, while phase modelling requires the use of accurate dispersion curves. Lithospheric models for large parts of the European-Mediterranean region have been published (*e.g.* Panza *et al.*, 1980; Calcagnile *et al.*, 1982; Snieder, 1988; Nesterof and Ianovskaia, 1988; Dost, 1990); however, an accurate 3-D structural model accounting for the structural complexity along a path from Iran to Italy over the wide frequency band of interest is not available.

Forward modelling (fig. 4), shows that a moment tensor solution obtained at low frequency (5-7 mHz) can reproduce the amplitude spectra in the wide frequency range 8-26 mHz for the 1990 mainshock. Only at frequencies approaching the corner frequency of this large event, with a centroid half-duration of 15 s (Dziewonski *et al.*, 1991), are significant amplitude discrepancies observed. If the phase of the synthetic spectra is corrected with smoothed phase shifts derived from the data spectra, the fit between data and synthetics in time domain is good across the frequency band of interest.

To model the complete waveforms of the mainshock and of the smaller aftershocks in the 10-30 mHz frquency band we derive group and phase velocity dispersion curves from records of the June 20 mainshock using two different approaches:

1) we compute phase velocity dispersion curves for Rayleigh and Love fundamental modes by smoothing the phase delays observed in waveform modelling (fig. 4);

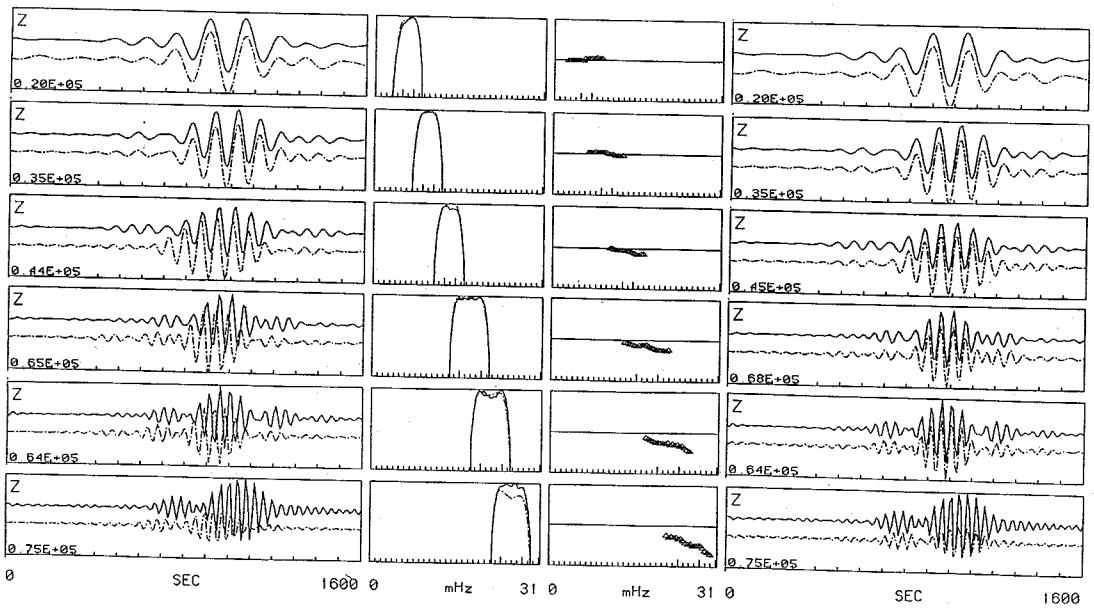

Fig. 4. Multiple-frequency forward modelling for the vertical component of station VSL. To the left are the comparisons of data and synthetics computed for the reference model (PREM) in five narrow frequency bands (from top to bottom 8-10, 10-14, 14-18, 18-22, 22-26) and in the whole 8-26 mHz band. The panels in the middle show the corresponding amplitude spectra for data and synthetics (the vertical logarithmic scale spans three orders of amplitude) and the phase difference between the complex spectra of data and synthetics (on a scale of $\pm 4\pi$); to the right are the fit obtained by correcting the path with the smoothed phase difference curve.

2) we calibrate group velocity dispersion curves for Rayleigh and Love fundamental modes using a standard time-frequency analysis, the Multiple Filter Technique of Herrmann (1987).

3.1. *Calibration of phase velocity dispersion*

With reliable source mechanism and duration available from low-frequency (5-7 mHz) moment tensor inversion, we derive the phase velocity for fundamental surface waves along each path, by smoothing the phase difference between the spectra of data and synthetics across the frequency band of interest. Locating the long-period space-time centroid of the source is essential for large earthquakes, to avoid contaminating the phase velocity calibration (*cfr.* Nakanishi and Kanamori, 1982). In a single station scheme, a normalization must be introduced; we set the phase velocity at 10 mHz to coincide with that predicted by a global standard model like PREM, a condition largely verified in practice at regional distances (Kulhanek, 1990) and in global tomographic inversions (Ekström, 1994; personal comunication).

We derive separate phase corrections from the radial, vertical and transversal components to obtain smoothed dispersion curves of Rayleigh and Love fundamental modes. To test for the stability of the phase corrections, we derive the calibrations for different events in the same sequence and apply them to smaller events.

3.2. *MFT calibration of group velocity dispersion*

The Multiple Filter Technique (MFT) was first introduced for the determination of group velocities of dispersed signals (Dziewonski *et al.*, 1969; Dziewonski and Hales, 1972). The MFT has been extensively used, for example to estimate modal spectral amplitudes (Herrmann, 1973), for source studies (Mills and Fitch, 1977; Herrmann *et al.*, 1981), for determination of Q structure (Cheng and Mitchell, 1981) and to measure the ellipticity of Rayleigh waves (Saxton *et al.*, 1977). Herrmann (1987) implemented the MFT in his program package for surface waves analysis.

In the MFT, a gaussian filter $H(\omega)$, defined as

$$H(\omega) = \begin{cases} e^{(-\alpha(\omega-\omega_0)^2/\omega_c^2)} & |\omega-\omega_0| \le \omega_c \\ 0 & |\omega-\omega_0| > \omega_c \end{cases} \qquad (3.1)$$

where $\omega_c = \omega_0(\pi/\alpha)^{\frac{1}{2}}$, is applied to the Fourier transform $A(\omega, r)e^{-j(k(\omega)r-\phi)}$ of a dispersive waveform that propagates at distance r from the source.

The envelope of the filtered time signal has the form

$$g(t, r) = \frac{A(\omega_0, r)}{2\pi}\omega_0\left(\frac{\pi}{\alpha}\right)e^{(-\omega_0(t-r/U_0)^2/4\alpha)} \qquad (3.2)$$

and will reach its maximum at t^*, travelling with group velocity $U = r/t^*$.

Dziewonski and Hales (1972), using MFT on synthetic seismograms, showed that group velocity determination by MFT has systematic errors when the group velocity changes rapidly with frequency; this error can be reduced by increasing α in the equations above, but a large α affects the temporal resolution of interfering modes (Herrmann, 1973). The problem of spectral biasing due to frequency domain filtering of surface wave seismograms has been investigated in detail by Russel *et al.* (1988). After some experimentation, we opted for a frequency independent $\alpha = 4\pi$, yielding $\omega_c = \omega_0/2$.

In fig. 5 we show the dispersion diagram for the vertical component of VSL station for the 1990 Iran mainshock obtained using the MFT. The dispersion of the fundamental Rayleigh mode is clearly visible; group velocities overlap those predicted by PREM in the 8-17 mHz frequency windows but are significantly lower at higher frequencies.

We find that the MFT discriminates efficiently between Love and Rayleigh fundamental modes and improves the capability of discriminating between surface and body wave signals arriving with the same group velocity.

As we need phase calibration for the waveform inversion, we derive phase velocity dispersion curves from the group velocity curves by requiring that the phase velocity be equal to the PREM at 10 mHz.

Figure 6a-c summarizes the results obtained for phase and group velocity dispersion for the VSL recordings of the 1990 Iran mainshock. In fig. 6a,b we compare group velocity dispersion curves for fundamental Rayleigh and Love waves from PREM and for typical oceanic and

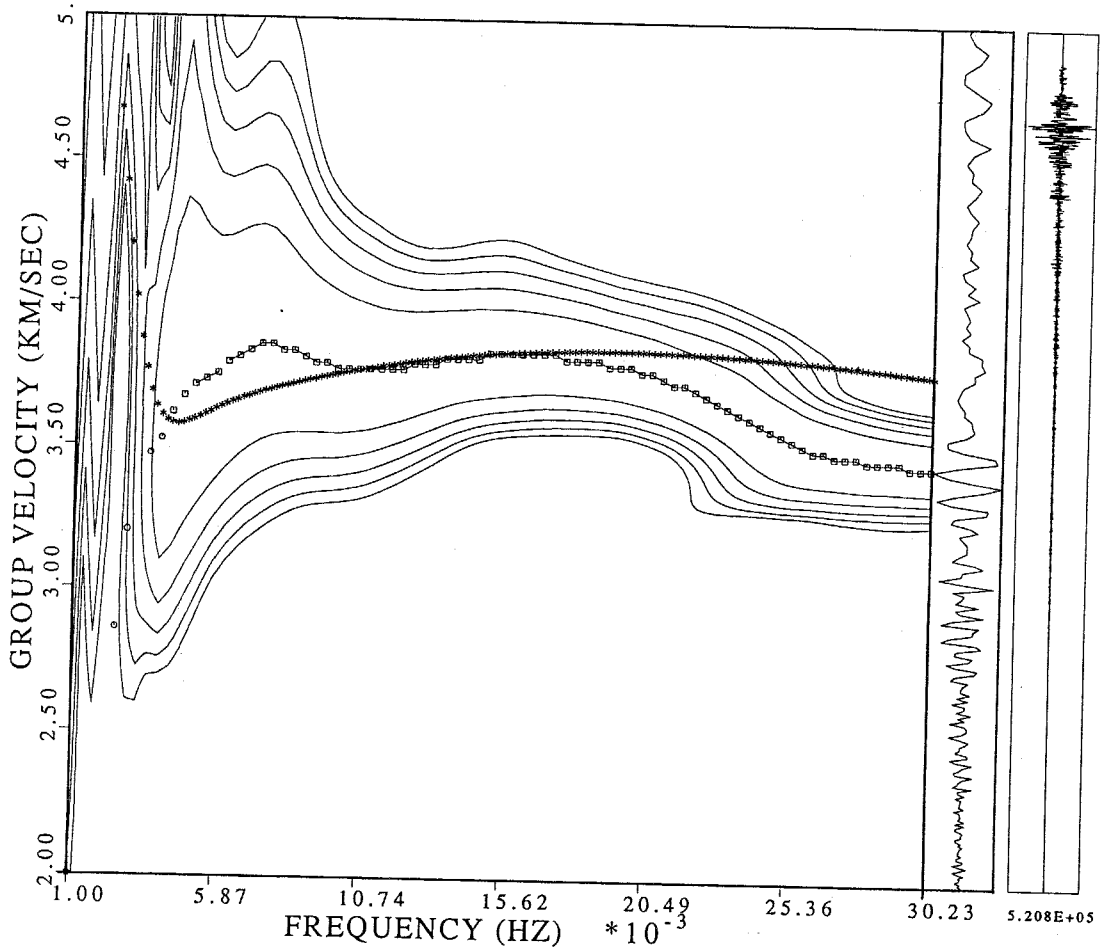

Fig. 5. Dispersion diagram of the vertical component of the VSL recording of the 1990 mainshock, obtained using the MFT algorithm of Herrmann (1987). The left panel contains the dispersion diagram windowed in the 2-5 km/s group velocity range and 1-30 mHz frequency range. Contours outline the portion of the spectrum with the largest arrivals; squares identify the group velocity of the dominating wave for each frequency. The right panels display the seismograms with time and group velocity. For comparison, the PREM dispersion curve for fundamental Rayleigh waves is shown with a thick line.

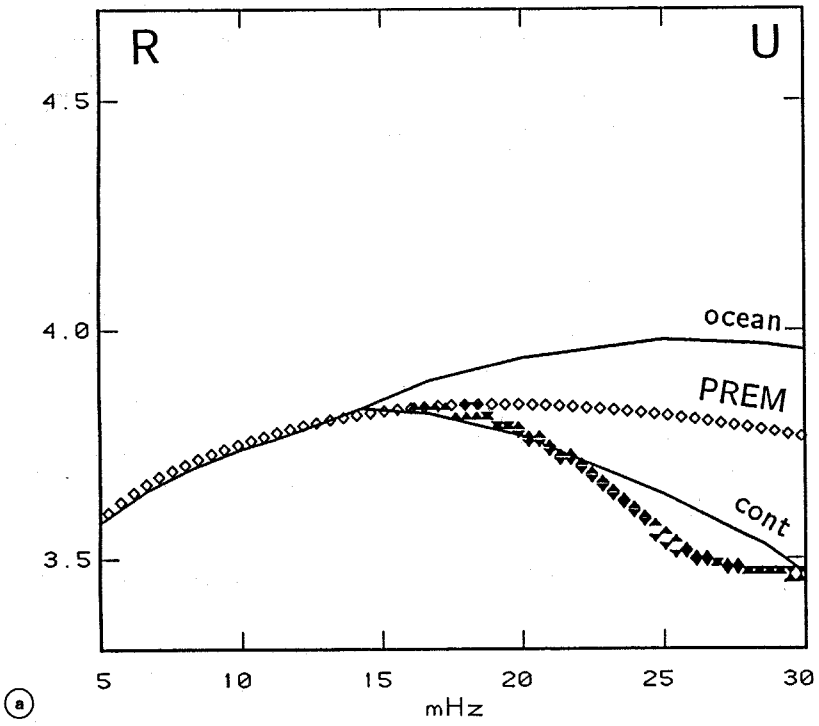
R
U
4.5
4.0
3.5
ocean
PREM
cont
5
10
15
20
25
30
mHz

(a)

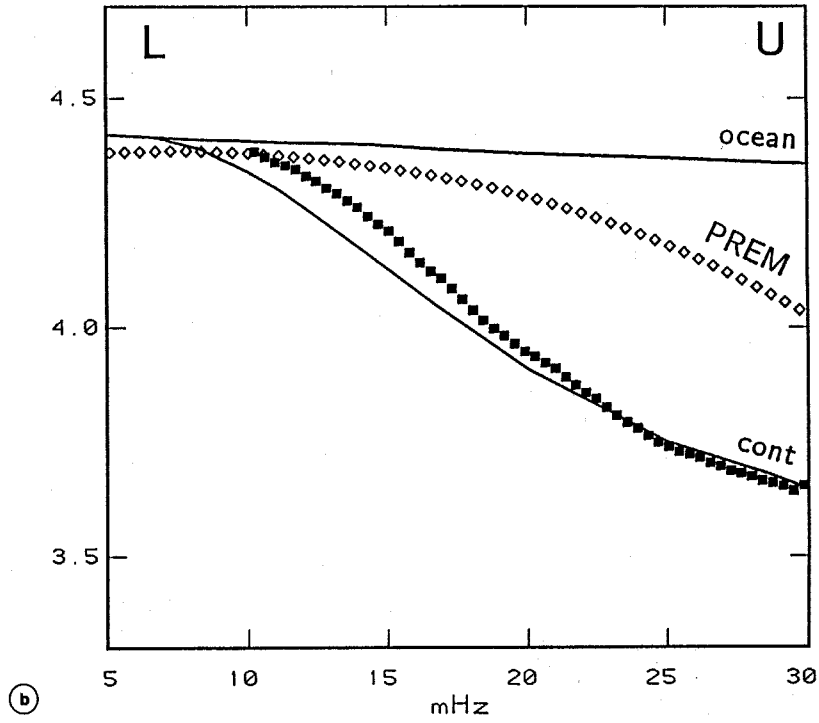
L
U
4.5
4.0
3.5
ocean
PREM
cont
5
10
15
20
25
30
mHz

(b)

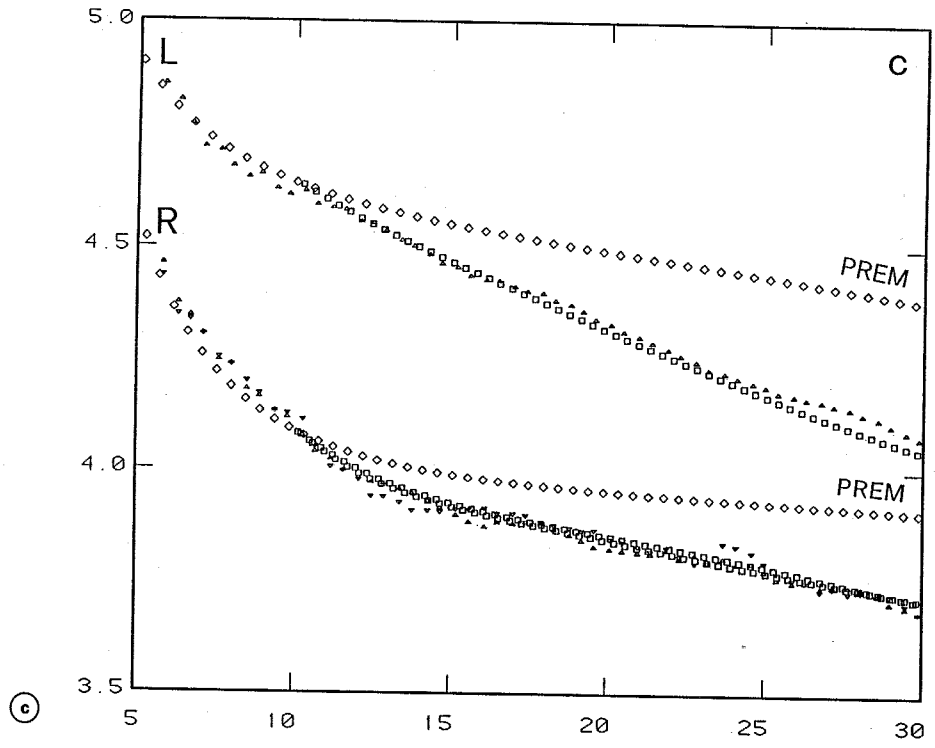

Fig. 6a-c. a) Group velocity dispersion curves for fundamental Rayleigh waves from PREM (diamonds), for typical oceanic (upper line) and continental (lower line) paths (modified from Kulhanek, 1990) and derived for the VSL vertical (upper triangle) and radial (lower triangle) components using the Multiple Filter Technique. b) Group velocity dispersion curves for fundamental Love waves from PREM (diamonds), for typical oceanic (upper line) and continental (lower line) paths (Kulhanek, 1990) and derived for the VSL transverse component (squares) using the Multiple Filter Technique. c) Phase velocity dispersion curves for fundamental Love waves (upper curves) and Rayleigh waves (lower curves) from PREM (diamonds) and those derived for the VSL transverse radial, and vertical components using MFT (squares); the unsmoothed phase delays of the 1990 mainshock are indicated with triangles.

continental paths with those derived using MFT; the observed Rayleigh and Love group velocities follow quite closely the dispersion curve of a typical continental path (the Rayleigh waves group velocities are even lower around 25 mHz frequencies). Indeed, the path followed by the surface waves from the Alborz mountains to the Sardinia Island follows the lower Atlas and the Anatolian plate before crossing a more complex region including the lower Dinarides, the Adriatic microplate, the Apennines and the Tyrrhenian Sea; of these tectonic blocks, only the Tyrrhenian Sea has a clear oceanic structure.

In fig. 6c we compare phase velocity dispersion curves for Rayleigh and Love fundamental modes from PREM with those derived using MFT and with the unsmoothed phase delays of the 1990 mainshock. The MFT curves produce an excellent fit to the unsmoothed phase delays of the 1990 mainshock, confirming that the phase velocities derived directly from waveform fitting are not contaminated by body waves arrivals.

The propagation of surface waves along a major arc is assumed in our approach; focussing and defocussing of surface wave paths due to lateral heterogeneities in velocity and Q can produce large amplitude effects at higher frequency, requiring 2-D and 3-D modelling (*e.g.* Snieder, 1988). These effects, however, are negligible at regional distances and in the frequency range considered.

4. Wide-band moment tensor inversion of the 1990 sequence

Using the phase velocity dispersion curves for Rayleigh and Love fundamental modes shown in fig. 6a-c, we adjust the phase of the Rayleigh and Love fundamental modes in our kernels and invert for the moment tensor of the mainshock and aftershocks of the Iran 1990 sequence from the VSL three-component records filtered in narrow and wide frequency bands.

Figures 7 to 9 display the results for the June 20, June 21 and June 24 events; the seismic moment and the frequency band used are indicated for each solution and the Harvard CMT solution is shown for comparison.

We obtain very stable results for the June 20 mainshock over the whole 8-30 mHz band; only at frequencies above 26 mHz, as explained before, do we observe minor amplitude contamination due to the large dimensions and long duration of this event. Comparable results are obtained using frequency bands as narrow as 2 mHz. The seismic moment ($M_0 = 1.56 \times 10^{27}$ dyne-cm) in the single station inversions is higher than the value obtained using uncalibrated multiple stations (*cfr.* the Harvard CMT estimate of 1.35×10^{27} dyne-cm). As the focal geometry we obtain in the same obtained in the multiple-station CMT, this effect is attributed to the accurate phase and amplitude match achieved in the single station inversion, resulting in misfit ratios better than 0.05 for noise-free records and, barring minor site amplification factors, in a reliable seismic moment estimate. The variation of seismic moment in different inversions (fig. 7) correspond to $M_w = 7.3$-7.5, and is comparable to the spread observed in the multi-stations CMT solutions obtained by other authors.

Similar consistency in narrow-band and wide-band inversions is achieved also for the June 21 (fig. 8) and June 24 (fig. 9) aftershocks. We obtain values of $M_0 = 3.9 \times 10^{24}$ dyne-cm ($M_W = 5.7$) for the June 21 event and $M_0 = 1.0 \times 10^{24}$ dyne-cm ($M_W = 5.3$) for the June 24 event in good agreement with the Harvard CMT solutions.

In figs. 8 and 9 we display the full moment tensor for our solutions and the CMTs. For the June 21 event this is done to show the consistency of our results across the whole 10-30 mHz band and the similarity with the CMT solution. For the June 24 event there is a discrepancy between the Harvard CMT best double couple, a pure strike-slip similar to the mainshock, and our best double couple, a reverse mechanism very similar to that of the June 21 event (fig. 1). This discrepancy is only illusional, as both our and the Harvard moment tensors are characterized by consistent deviation from a pure double couple mechanism. The full moment tensor plots of fig. 9 show the solutions to be in good agreement.

5. Conclusions

We present a method for the inversion of complete waveforms in the 5-30 mHz frequency band for moment tensor determination. The method is based on the calibration of phase and group velocity dispersion curves for Rayleigh and Love fundamental modes to account for heterogeneous lithospheric structure, using (a) group velocities obtained with the Multiple Filter Technique and (b) smoothed phase delays obtained from waveform modelling of the mainshock. We observe substantial agreement between the phase calibrations obtained following these two complementary approaches.

The method is applied to the analysis of single station records of the VSL MEDNET station for the 1990 NW Iran earthquake sequence (the events of June 20, 21 and 24), obtaining a revised seismic moment of the June 20, 1990 Iranian earthquake $M_0 = 1.56 \times 10^{27}$ dyne-cm ($M_W = 7.4$).

The method proves to be a very robust tool

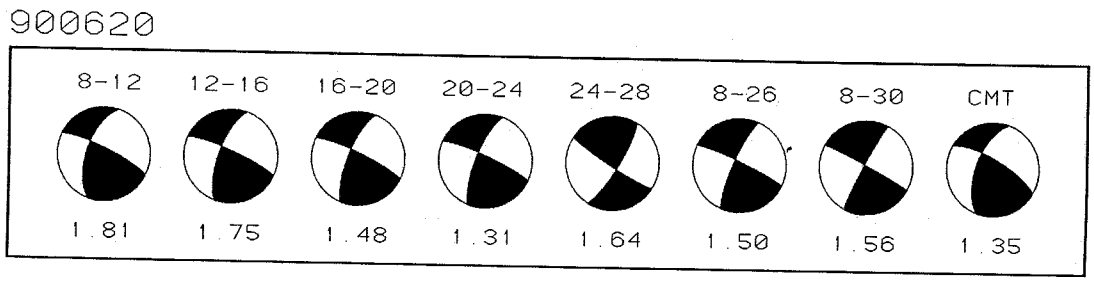

Fig. 7. Narrow-band and wide-band moment tensor solutions for the June 20, 1990 Iran mainshock, obtained introducing the calibrated phase velocity dispersion curves for Rayleigh and Love fundamental waves (fig. 6a-c). For each solution we show the best double-couple focal mechanism and we indicate the frequency band used in the inversion (above) and the seismic moment in units of 10^{27} dyne-cm (below). For comparison the CMT solution is also shown (Dziewonski *et al.*, 1991).

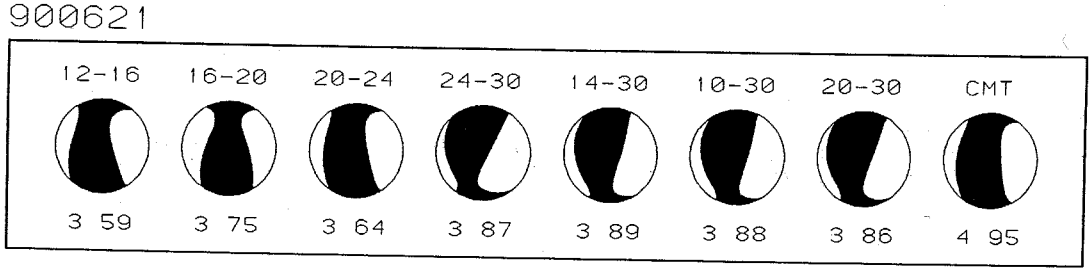

Fig. 8. Narrow-band and wide-band moment tensor solutions for the June 21, 1990 Iran aftershock, obtained introducing the calibrated phase velocity curves for Rayleigh and Love fundamental waves (fig. 6a-c). We show the full moment tensor solutions and we indicate the frequency band used in the inversion (above) and the seismic moment in units of 10^{24} dyne-cm (below). For comparison the CMT solution is also shown (Dziewonski *et al.*, 1991).

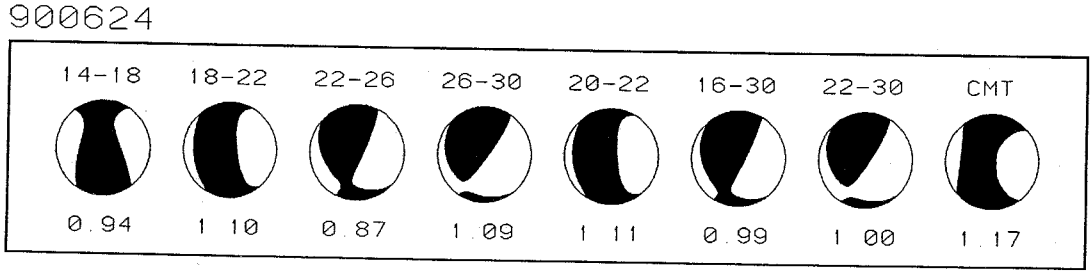

Fig. 9. Narrow-band and wide-band moment tensor solutions for the June 24, 1990 Iran aftershock, obtained introducing the calibrated phase velocity curves for Rayleigh and Love fundamental waves (fig. 6a-c). We show the full moment tensor solutions and we indicate the frequency band used in the inversion (above) and the seismic moment in units of 10^{24} dyne-cm (below). For comparison the CMT solution is also shown (Dziewonski *et al.*, 1991).

for the analysis of moderate and large earthquakes at regional distances, producing consistent moment tensor solutions from single station inversions in narrow (2-4 mHz) and wide (up to 20 mHz) frequency bands across the whole band of interest.

Acknowledgements

D.G. is grateful to J. Woodhouse for initiating him to the art of handling the Earth's normal modes, and to A.M. Dziewonski and J.H. Woodhouse for the experience gained on the CMT method while at Harvard University. L.M. is grateful to R.B. Herrmann for the assistance in using MFT. We thank H. Kanamori and J. Boatright for useful insight and comments.

The work was conducted at the Istituto Nazionale di Geofisica of Roma. The MEDNET Data Center is commended for collecting and promptly making the digital data available to the seismological community. We acknowledge the leading role of the WorldLab in the deployment of MEDNET.

REFERENCES

BERBERIAN, M., M. QORASHI, J.A. JACKSON, K. PRIESTLEY and T. WALLACE (1992): The Rudbar-Tarom earthquake of 20 June 1990 in NW Persia: preliminary field and seismological observations, and its tectonic significance, *Bull. Seismol. Soc. Am.*, **82**, 1726-1755.

BOSCHI, E., D. GIARDINI and A. MORELLI (1991): MedNet: the broad-band seismic network for the Mediterranean, *Il Cigno Galileo Galilei*, Roma.

CALCAGNILE, G., F. D'INGEO, P. FARRUGIA and G.F. PANZA (1982): The lithosphere in the Central Eastern Mediterranean Area, *Pure Appl. Geophys.*, **120**, 389-406.

CHENG, C.C. and J. MITCHELL (1981): Crustal Q structure in the United States from multi-mode surface waves, *Bull. Seismol. Soc. Am.*, **71**, 161-181.

DOST, B. (1990): Upper mantle structure under Western Europe from fundamental and higher mode surface waves using the NARS array, *Geophys. J. Int.*, **100**, 131-151.

DREGER, D.S. and D. HELMBERGER (1990): Broadband modelling of local earthquakes, *Bull. Seismol. Soc. Am.*, **80**, 1162-1179.

DUFUMIER, H. and M. CARA (1995): On the limits of linear moment tensor inversion of surface wave spectra, *Pure App. Geophys.* (in press).

DZIEWONSKI, A.M., S. BLOCH and M. LANDISMANN (1969): A technique for the analysis of transient seismic signals, *Bull. Seismol. Soc. Am.*, **59**, 427-444.

DZIEWONSKI, A.M. and A.L. HALES (1972): Numerical analysis of dispersed seimic waves, edited by B. BOLT, *Methods Comput. Phys.*, **11**, 39-85.

DZIEWONSKI, A.M. and D.L. ANDERSON (1981): Preliminary Reference Earth Model (PREM), *Phys. Earth Planet. Int.*, **25**, 297-356.

DZIEWONSKI, A.M., T.A. CHOU and J.H. WOODHOUSE (1981): Determination of earthquake source parameters from waveform data for studies of global and regional seismicity, *J. Geophys. Res.*, **86**, 2825-2852.

DZIEWONSKI, A.M., G. EKSTRÖM, J.H. WOODHOUSE and G. ZWART (1991): Centroid-moment tensor solutions for April-June 1990, *Phys. Earth Planet. Int.*, **66**, 133-143.

EKSTRÖM, G., A.M. DZIEWONSKI and J.M. STEIM (1986): Single station CMT: application to the Michoacan, Mexico, earthquake of September 19, 1985, *Geophys. Res. Lett.*, **13**, 173-176.

FUKUSHINA, T., D. SUETSUGU, I. NAKANISHI and I. YAMADA (1989): Inversion for near earthquakes using long-period digital seismograms, *J. Phys. Earth*, **37**, 1-29.

GIARDINI, D. (1992): Moment tensor inversion from MedNet data: (1) large worldwide earthquakes of 1990, *Geophys. Res. Lett.*, **19**, 713-716.

GIARDINI, D., E. BOSCHI, S. MAZZA, A. MORELLI, D. BEN SARI, D. NAJID, H. BENHALLOU, M. BEZZEGHOUD, H. TRABELSI, M. HAFAIED, R. KEBEASY and E. IBRAHIM (1992): Very-broad-band seismology in Northern Africa under the MedNet project, *Tectonophysics*, **209**, 17-30.

GIARDINI, D., E. BOSCHI and B. PALOMBO (1993): Moment tensor inversion from MedNet data: (2) earthquakes of the Mediterranean, *Geophys. Res. Lett.*, **20**, 273-276.

GIARDINI, D., B. PALOMBO and N.A. PINO (1995): Long-period modelling of Mednet waveforms for the December 13, 1990 Eastern Sicily earthquake, *Annali di Geofisica* (in press).

HERRMANN, R.B. (1973): Some aspects of band-pass filtering of surface waves, *Bull. Seismol. Soc. Am.*, **63**, 663-671.

HERRMANN, R.B. (1987): *Computer Programs in Seismology, User's manual* (St. Louis University, Missouri), vol. II.

HERRMANN, R.B., S.K. PARK and C.Y. WANG (1981): The Denver earthquakes of 1967-68, *Bull. Seismol. Soc. Am.*, **71**, 731-745.

HOLT, W.E. and T.C. WALLACE (1987): A procedure for the joint inversion of regional and teleseismic long-period body waves, *Geophys. Res. Lett.*, **14**, 903-906.

JIMENEZ, E., M. CARA and D. ROULAND (1989): Focal mechanisms of moderate-size earthquakes from the analysis of single-station three component surface wave records, *Bull. Seismol. Soc. Am.*, **79**, 955-972.

KANAMORI, H. and J.W. GIVEN (1981): Use of long-period surface waves for rapid determination of earthquakes-source parameters, *Phys. Earth Planet. Int.*, **11**, 312-332.

KULHANEK, O. (1990): *Anatomy of seismograms* (Elsevier Science Publishers B. V.).

MILLS, J.M. and T.J. FITCH (1977): Thrust faulting and crust-mantle structure of East Australia, *J. Geophys. Res.*, **48**, 351-384.

MOINFAR, A.A. and A. NADERZADEH (1990): *An immediate and preliminary report on the Manjil, Iran earthquake of 20 June 1990*, Building and Housing Research Center, Ministry of Housing and Urban Development, **119**, 68.

NAKANISHI, I. and H. KANAMORI (1982): Effects of lateral heterogeneity and source process time on the linear moment tensor inversion of long period Rayleigh waves, *Bull. Seismol. Soc. Am.*, **72**, 2063-2080.

NAKANISHI, I., T. MORIYA and M. ENDO (1992): The November 13, 1990 earthquake off the coast of the Primorskij region, the Eastern Russia, *Geophys. Res. Lett.*, **19**, 549-552.

NESTEROF, A.N. and T.B. IANOVSKAIA (1988): Horizontal lithospheric heterogeneity in Southwestern Europe from surface wave observations (in Russian), *Rev. Russian Acad. Sci. Earth Sci.*, **11**, 3-16.

PANZA, G., S. MÜLLER and G. CALCAGNILE (1980): The gross features of the litosphere-astenosphere system in Europe from seismic surface waves and body waves, *Pure Appl. Geophys.*, **118**, 1209-1213.

RITSEMA, J. and T. LAY (1993): Rapid source mechanism determination of large ($M_w \geq 5$) earthquakes in the Western United States, *Geophys. Res. Lett.*, **20**, 1611-1614.

ROMANOWICZ, B. and G. SUAREZ (1983): On an improved method to obtain the moment tensor and depth of earthquakes from the amplitude spectrum of Rayleigh waves, *Bull. Seismol. Soc. Am.*, **73**, 1513-1526.

ROMANOWICZ, B., D. DREGER, M. PASYANOS and R. UHRHAMMER (1993): Monitoring of strain release in Central and Northern California using broadband data, *Geophys. Res. Lett.*, **20, 15**, 1643-1646.

RUSSELL, D.R., R.B. HERRMANN and H.J. WHANG (1988): Application of frequency variable filters to surface-waves amplitude analysis, *Bull. Seismol. Soc. Am.*, **78**, 339-354.

SAXTON J.L., A.J. RUDMAN and J. MEAD (1977): Ellipticity of Rayleigh waves in the Midwest, *Bull. Seismol. Soc. Am.*, **67**, 369-382.

SIPKIN, S.A. (1986): Estimation of earthquakes source parameter by the inversion of waveform data: global seismicity, 1981-1983, *Bull. Seismol. Soc. Am.*, **76**, 1515-1541.

SNIEDER, R. (1988): Large-scale waveform inversion of surface waves for lateral heterogeneity 2. Application to surface waves in Europe and the Mediterranean, *J. Geophys. Res.*, **93**, 12067-12080.

THIO, H.K. and H. KANAMORI (1995): Moment tensor inversions for local earthquakes using surface waves recorded at TERRAscope, *Bull. Seismol. Soc. Am.* (in press).

THIO, H.K., K. SATAKE, M. KIKUCHI and H. KANAMORI (1990): On the Sudan, Iran and Philippines earthquakes of 1990 (abstract), *EOS, Trans. AGU*, **71**, 1438.

WOODHOUSE, J.H. (1988): The calculation of eigenfrequencies and eigenfunctions of the free oscillations of the Earth and the Sun, in *Seismological Algorithms*, edited by D.J. DOORNBOS (Academic Press), 321-370.